ICCV
#3272

ICCV
#3272

ICCV 2019 Submission #3272. CONFIDENTIAL REVIEW COPY. DO NOT DISTRIBUTE.

Deep Constrained Dominant Sets
Supplementary Material

Anonymous ICCV submission

Paper ID 3272

In the supplementary material, we provide additional experiments on cross-dataset person-re-identification (re-id) using the proposed deep constrained dominant sets (DCDS) on Market1501 dataset. In section one, we summarize the datasets we used in our experiments. In section two, we present the experiments we have performed on cross-dataset person re-id. And, in section three, we provide hyper parameter analysis on DukeMTMC-reID and CUHK03 datasets. Figure 1 illustrates an example of our method training-output (left) and learning objective, target matrix, (right). Figure 2 demonstrates the similarity fusing process, between the V-Net and CDS-Net, alongside sample qualitative results.

1. Datasets

In multiple dataset (MD) setup, we first train our model on eight datasets: CUHK03 [4], CUHK01 [3], Market1501 [7], DukeMTMC-reID [9], Viper [1], MSMT17 [6], GRID [5], and ILIDS [8]. Next, we fine-tune and evaluate on each of CUHK03 [4], Market1501 [7], and DukeMTMC-reID [9] datasets.

2. Experiments on Cross-datasets Evaluation

Due to the lack of abundant labeled data, cross-dataset person re-id has attracted great interest. Recently, Fan *et al.* [2] have developed a progressive clustering-based method to attack cross-dataset person re-id problem. To further validate our proposed DCDS, we apply our method on cross-dataset person re-id problem and compare it with progressive unsupervised learning (PUL) [2]. To this end, we train our model on DukeMTMC-reID and CUHK03 datasets and test it on Market1501 dataset. We then compare it with PUL [2], which has also been trained on CUHK03 and DukeMTMC-reID datasets. As can be observed from Table 1, even though our proposed method is not intended for cross-dataset re-id, it has gained a substantial improvements over PUL [2], that was mainly designed to attack person re-id problem in a cross-dataset setup.
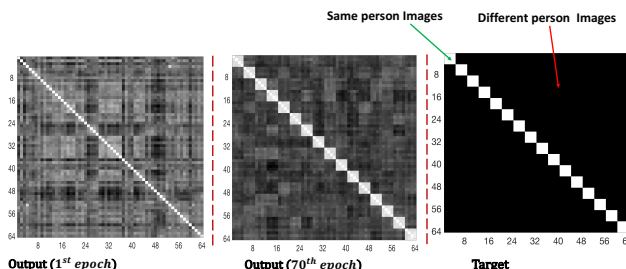

Figure 1. On the right hand side, the target matrix is shown. There are total 16 persons in the mini-batch and 4 images per ID ($\Omega = 4$), batch size = 64. In the target matrix, the white-blocks represent the similarity between the same person-images in the mini-batch, whereas the black-blocks of the matrix define the dissimilarities between different person images. In the similarity matrix shown left (after one epoch) and middle (after 70th epochs) each row of the output matrix denotes the fused similarity obtained from the CDS-Net and V-Net, per Equ. (6) in the main manuscript. Thus, we optimize our model until we obtain an output with a similar distribution of the target matrix. As can be seen, our model has effectively learned and gives a similarity matrix (shown in the middle) which is closer to the target matrix.

3. Parameter Analysis

Similar to the parameter analysis reported in the main manuscript, we report hyper parameter analysis on DukeMTMC-reID and CUHK03 dataset. The performance of our method with respect to the fusing parameters on DukeMTMC-reID and CUHK03 are shown in Figure 3 (a) and Figure 3 (b), respectively. Thereby, as can be observed, the results show similar phenomena as in Market1501, where the mAP increases with a larger β value. Figure 4 shows the similarity distribution given by the baseline and the proposed DCDS using three different probe-images, with a batch size of 64, and setting Ω to 4, 8 and 16.

ICCV
#3272

ICCV 2019 Submission #3272. CONFIDENTIAL REVIEW COPY. DO NOT DISTRIBUTE.
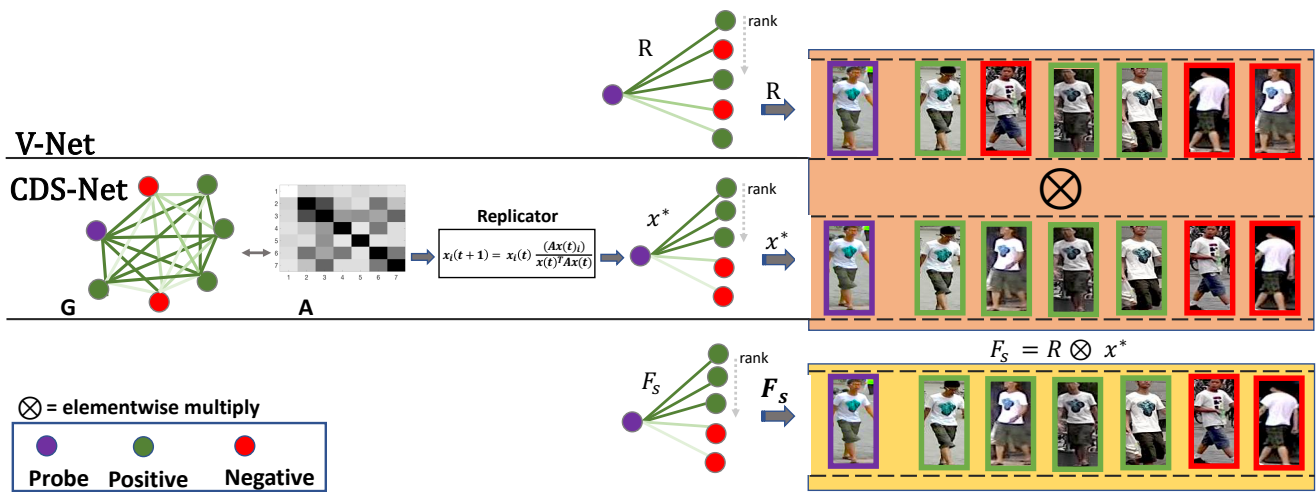
ICCV
#3272

Figure 2. Exemplar results obtained as a result of the similarity fusion between the V-Net and CDS-Net. The Upper-row shows the probe and gallery similarity (R) obtained from the V-Net, where the green circles show persons similar to the probe (shown by purple-circle), while the red circles denote persons different from the probe image. Middle-row shows the workflow in CDS-Net. First, graph G is formed using the similarity obtained from the dot products. We then construct the modified affinity matrix B, followed by application of replicator dynamics on A to obtain the probe gallery similarity (X^*). Finally, We elementwise multiply X^* and R to find the final probe-gallery similarity (F_s), shown in the third row. The intensity of the edges in, G, R, x^*, and F_s define the similarity value, where the bold ones denote larger similarity values, whereas the pale-edges depict smaller similarity values.
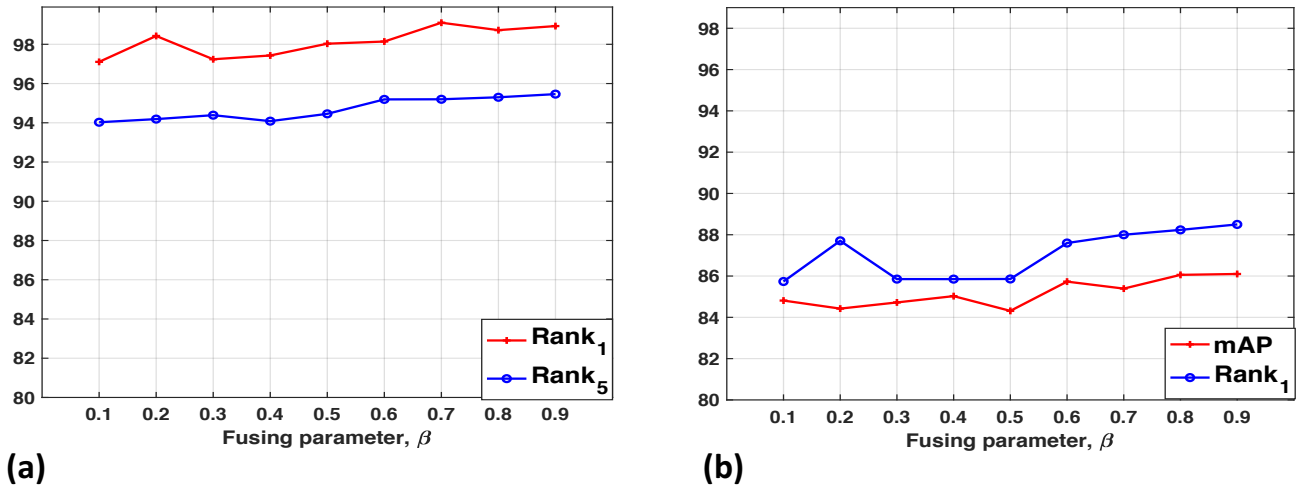

Figure 3. Performance of our model with respect to fusing parameter β, on (a) CUHK03, and (b) DukeMTMC-reID, datasets.

	Train on Duke, CUHK03 $\rightarrow$ **Test** on Market1501	
Methods	mAP	rank-1
PUL [2]	20.5	45.5
Ours	**24.5**	**51.3**

Table 1. A comparison of the proposed method with PUL [2] on Market1501 dataset.

ICCV
#3272

ICCV
#3272

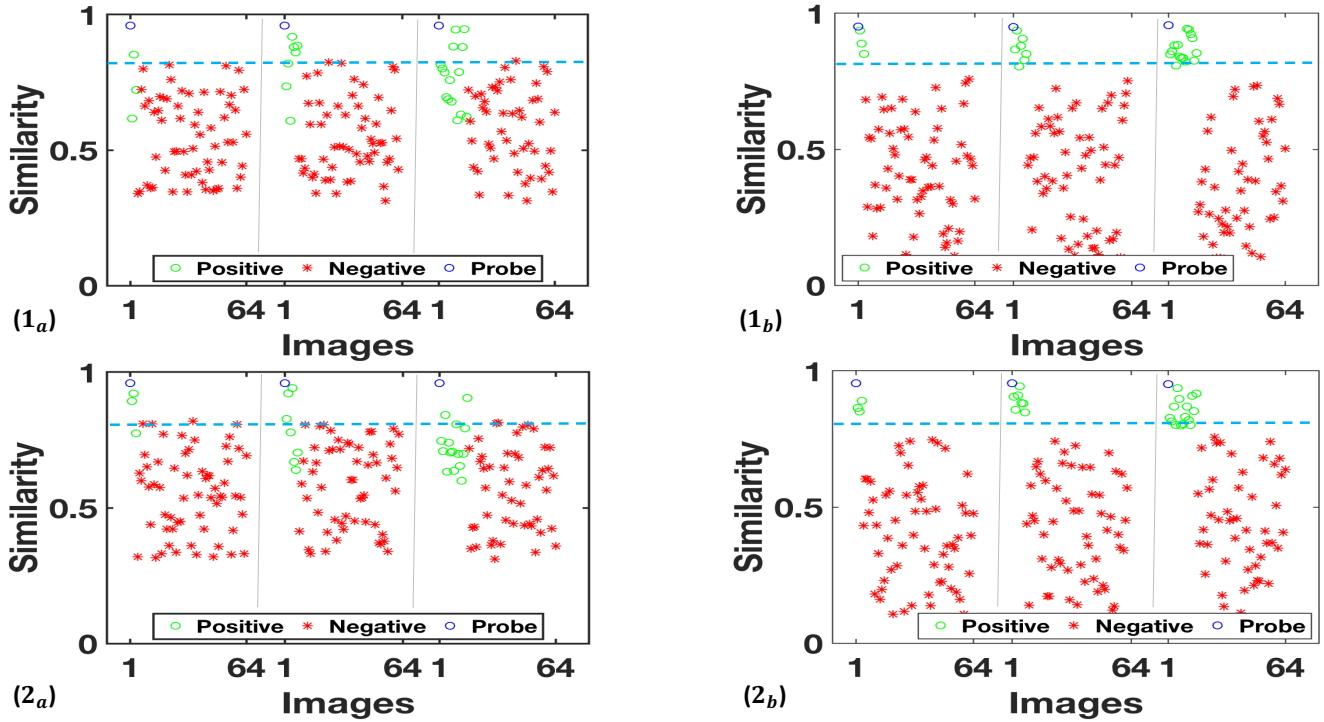ICCV 2019 Submission #3272. CONFIDENTIAL REVIEW COPY. DO NOT DISTRIBUTE.

Figure 4. Shows experimental analysis performed on CUHK03 $(1_{a,b})$, and DukeMTMC-reID $(2_{a,b})$ datasets. $1_a, 2_a$ and $1_b, 2_b$ illustrate the similarity between the probe-gallery images obtained from the baseline and DCDS method, respectively. It can be observed that the baseline method has assigned larger similarity values for false positive samples (red asterisks above the blue dashed-line) and smaller similarity values for false negative samples (green circles below the blue dashed-line). On the other hand, the proposed DCDS has efficiently assigned the appropriate similarity scores to the true positive and negative samples. Note that, for better visibility, we have randomly assigned a large (close to 1) self-similarity value to the probe (blue-circle).

ICCV
#3272

ICCV
#3272

ICCV 2019 Submission #3272. CONFIDENTIAL REVIEW COPY. DO NOT DISTRIBUTE.

References

[1] S. B. D. Gray and H. Tao. Evaluating appearance models for recognition, reacquisition. In *IEEE International workshop on performance evaluation of track- ing and surveillance,*, pages 31–44, 2007. 1

[2] H. Fan, L. Zheng, C. Yan, and Y. Yang. Unsupervised person re-identification: Clustering and fine-tuning. *TOMCCAP*, 14(4):83:1–83:18, 2018. 1, 2

[3] W. Li, R. Zhao, and X. Wang. Human reidentification with transferred metric learning. In *Computer Vision - ACCV 2012 - 11th Asian Conference on Computer Vision, Daejeon, Korea, November 5-9, 2012, Revised Selected Papers, Part I*, pages 31–44, 2012. 1

[4] W. Li, R. Zhao, T. Xiao, and X. Wang. Deepreid: Deep filter pairing neural network for person re-identification. In *CVPR*, pages 152–159. IEEE Computer Society, 2014. 1

[5] C. C. Loy, T. Xiang, and S. Gong. Multi-camera activity correlation analysis. In *CVPR*, pages 1988–1995. IEEE Computer Society, 2009. 1

[6] L. Wei, S. Zhang, W. Gao, and Q. Tian. Person transfer GAN to bridge domain gap for person re-identification. In *CVPR*, pages 79–88. IEEE Computer Society, 2018. 1

[7] L. Zheng, L. Shen, L. Tian, S. Wang, J. Wang, and Q. Tian. Scalable person re-identification: A benchmark. In *ICCV*, pages 1116–1124. IEEE Computer Society, 2015. 1

[8] W. Zheng, S. Gong, and T. Xiang. Associating groups of people. In *BMVC*, pages 1–11. British Machine Vision Association, 2009. 1

[9] Z. Zheng, L. Zheng, and Y. Yang. Unlabeled samples generated by GAN improve the person re-identification baseline in vitro. In *ICCV*, pages 3774–3782. IEEE Computer Society, 2017. 1